Journal of Power Sources 222 (2013) 225–229

Contents lists available at SciVerse ScienceDirect

Journal of Power Sources

journal homepage: www.elsevier.com/locate/jpowsour

Short communication

Single-crystalline rutile TiO_2 nanowires for improved lithium ion intercalation properties

Biao Han [a], Si-Jin Kim [a], Bo-Mi Hwang [a], Seong-Bae Kim [a,b], Kyung-Won Park [a,*]

[a] Department of Chemical Engineering, Soongsil University, Seoul 156-743, Republic of Korea
[b] Daejung Energy Materials Co., Ltd., Iksan, Republic of Korea

HIGHLIGHTS

- TiO_2 nanowires for lithium ion batteries were synthesized by hydrothermal process without any surfactant and template.
- The single-crystalline nature of rutile TiO_2-NWs grown along the [001] direction was clearly observed.
- The single-crystalline rutile TiO_2-NWs showed improved charge capacity and high-rate performance.

ARTICLE INFO

Article history:
Received 25 May 2012
Received in revised form
22 August 2012
Accepted 24 August 2012
Available online 3 September 2012

Keywords:
Single-crystalline
Rutile
TiO_2
Nanowire
Lithium intercalation

ABSTRACT

We report single-crystalline TiO_2 nanowires (TiO_2-NWs) synthesized by hydrothermal process without any surfactant and template with enhanced lithium intercalation properties. The single-crystalline nature of rutile TiO_2-NWs was clearly observed by field-emission transmission electron microscopy and fast Fourier transform pattern demonstrating that the nanowire growth is along the [001] direction. The single-crystalline rutile TiO_2-NWs showed much higher charge capacity and excellent high-rate performance as compared to typical rutile TiO_2 nanoparticles. The improved lithium-ion intercalation properties of TiO_2-NWs may be attributed to relatively large specific surface area, short transport distance of 1-D nanostructure, and freedom for volume change accompanied by lithium-ion intercalation.

1. Introduction

Rechargeable lithium-ion batteries (LIBs) are essential portable power sources because of their high-energy density, high voltage, long cyclability, and high-power density [1,2]. Until now, graphite-based materials have been utilized as a typical anode material for the commercial LIBs. Since the graphite anode materials have several disadvantages, however, such as structural deformation and initial loss of capacity, it is quite urgent to develop the new materials with high performance and simple electrode fabrication method [3,4]. In general, titanium dioxide (TiO_2) has been widely studied as a representative engineering material in a variety of applications such as photocatalytic activity [5,6], catalyst supports [7] and gas sensors [5–8]. Furthermore, TiO_2 is regarded as a promising lithium insertion/extraction material with low production cost and high capacity for lithium intercalation [9].

One-dimensional (1-D) TiO_2 nanostructured materials such as nanorods, nanowires, and nanotubes have been focused on in order to achieve advanced LIBs with high energy density, large capacity, high rate performance and long cycle life, because of fast electronic/ionic transport and relaxation of the strain during Li intercalation process [10,11]. Recently, considerable effort has been focused on exploring diverse synthetic methods ranging from vapor-phase techniques to solution-growth processes for the synthesis of 1-D nanostructure TiO_2 [12–15]. In particular, in the case of nanobelts or nanotubes, it is well known that various types of TiO_2 nanostructures can be synthesized through strong acid treatment under hydrothermal or non-hydrothermal conditions [16–20]. Among the one-dimensional nanostructures, the nanowire electrode shows particular properties such as rapid electron collection of carriers and charge transport assisted by its one-dimensional structure [21–25]. Recently, it has been reported that three-step hydrothermal method was developed for growing oriented single-crystalline TiO_2-B and/or anatase TiO_2 nanowire arrays on titanium foil [26].

* Corresponding author. Tel.: +82 2 820 0613; fax: +82 2 812 5378.
E-mail address: kwpark@ssu.ac.kr (K.-W. Park).

0378-7753/$ – see front matter © 2012 Elsevier B.V. All rights reserved.
http://dx.doi.org/10.1016/j.jpowsour.2012.08.073

Herein, we synthesized single-crystalline rutile TiO_2-NWs for LIBs via hydrothermal process without any surfactant and template. The structural characterization of the TiO_2-NW was carried out using high-resolution transmission electron microscopy (HR-TEM), fast Fourier transform (FFT), X-ray diffraction (XRD) analysis, and nitrogen sorption measurement. To evaluate the performance for LIBs, charge-discharge and rate cycling curves of the electrodes were measured using a lithium coin cell.

2. Experimental

2.1. Synthesis

For TiO_2-NWs, 8 mL of titanium(IV) isopropoxide (TTIP (97 wt.%), Aldrich) was dropped in 40 mL of 5 M hydrochloric acid (HCl (36 wt.%), Aldrich) with constant stirring at 25 °C for 1 h and then kept at 120 °C for 12 h. After the hydrothermal process, the resulting precipitates were cooled to room temperature, washed several times with ethanol and distilled water, and then precipitated using a centrifuge at 9000 rpm. The white TiO_2 powders were obtained after drying in a 60 °C oven.

2.2. Structural analysis

X-ray diffractometer (XRD) analysis was carried out using Rigaku XRD with Cu K_α ($\lambda = 0.15{,}418$ nm) source with a Ni filter. The source was operated at 40 kV and 100 mA. The 2θ angular scan from 20° to 60° was explored at a scan rate of 5° min^{-1}. The resolution in the scans was kept at 0.02°. The morphology and size distribution of the samples were characterized by Field Emission Transmission Electron Microscope (FE-TEM) (a Tecnai G2 F30 system) operating at 300 kV. Transmission Electron Microscope (TEM) samples were prepared by placing drops of powder suspension dispersed in ethanol on a carbon-coated copper grid. Nitrogen adsorption and desorption isotherms were measured at 77 K using a Micromeritics ASAP 2020. Before the adsorption measurements, all samples were outgassed at 473 K for 360 min in the port of the adsorption analyzer. The starting relative pressure was 0.995 P/P^o and ending relative pressure was 0.01 P/P^o.

2.3. Preparation of the electrodes

The electrodes were prepared by mixing 70 wt.% TiO_2 as an active material, 20 wt.% acetylene black as a conducting agent, and 10 wt.% polyvinylidene fluoride (PVDF) as a binder. In order to obtain the slurry, several drops of N-methylpymolidinone were added into the mixture of nanowires with graphite and PVDF. The prepared slurry was homogenized by stirring and then coated uniformly on 11 μm thick copper foil substrates. The electrode dried in an oven at 80 °C for 12 h and then cooled down to room temperature. The cells were assembled in a high purity argon filled glove box using the TiO_2-NWs as the working electrode and lithium foil as the counter and reference electrodes and a separator that was saturated with the electrolyte solution that consisted of 1.1 M

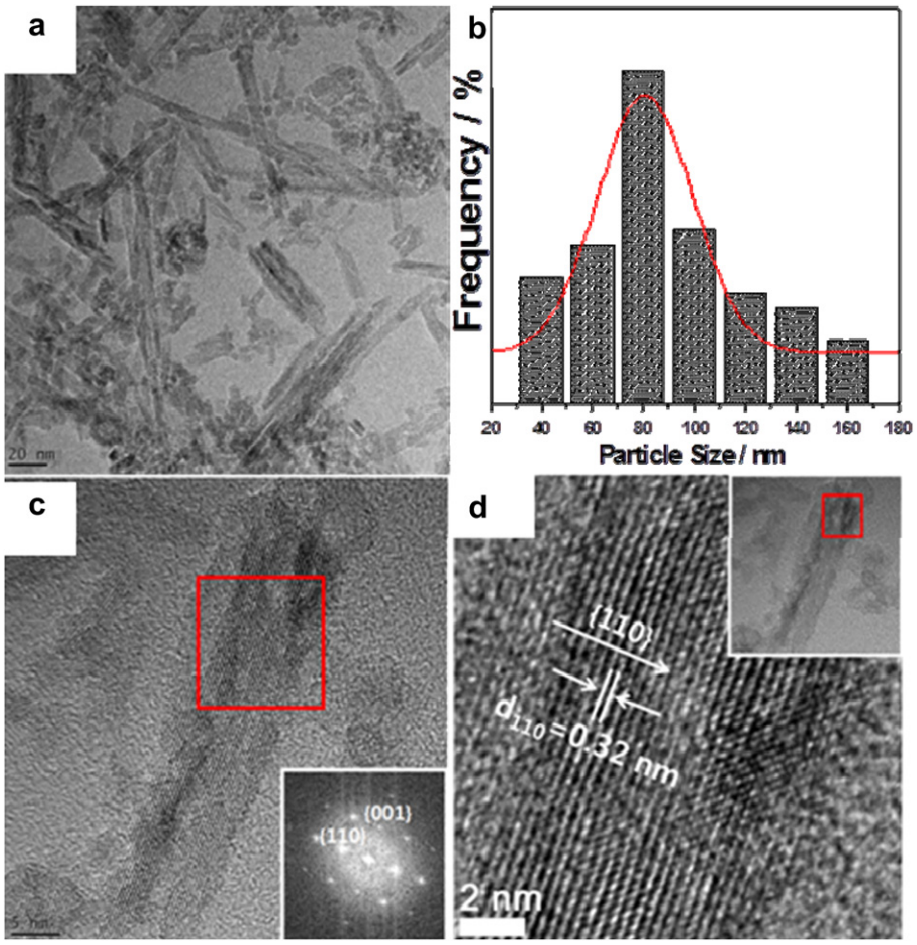

Fig. 1. (a) TEM image of TiO_2-NWs; (b) Size-distribution histogram of TiO_2-NWs; (c) TEM image of a TiO_2-NW(The inset indicates the corresponding FFT pattern.); (d) HR-TEM image of a TiO_2-NW(The inset indicates the TEM image.).

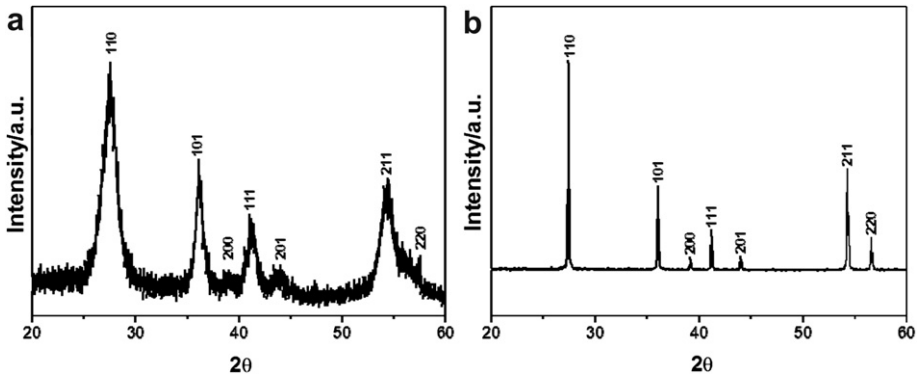

Fig. 2. (a) Wide-angle XRD pattern of TiO_2 NWs and (b) TiO_2 NPs prepared by heating commercial TiO_2 (Degussa P25) at 800 °C in air atmosphere.

$LiPF_6$ dissolved in a mixture of ethylene carbonate (EC) and dimethyl carbonate (DMC) with a volume ratio of EC/DMC = 1:1.

2.4. Electrochemical measurement

The electrochemical properties of the assembled cells were recorded with charge/discharge curves in a voltage window between 3.0 and 1.0 V. The charge/discharge tests were galvanostatically cycled between 3.0 and 1.0 V for 100 cycles at a current rate of 1 C. These charge/discharge tests were also performed at various current rates from 0.5 to 20 C in order to confirm the rate capability. All of the electrochemical measurements were completed at room temperature.

3. Results and discussion

Fig. 1(a) and (b) show that the average diameter and length of the as-synthesized TiO_2-NWs are 8.9 and 80.8 nm, respectively. The HR-TEM image and corresponding FFT pattern of a TiO_2-NW (Fig. 1(c) and (d)) confirm the single-crystalline nature of the nanowire and also demonstrate that the nanowire growth is along the [001] direction. Powder XRD pattern of the TiO_2-NWs

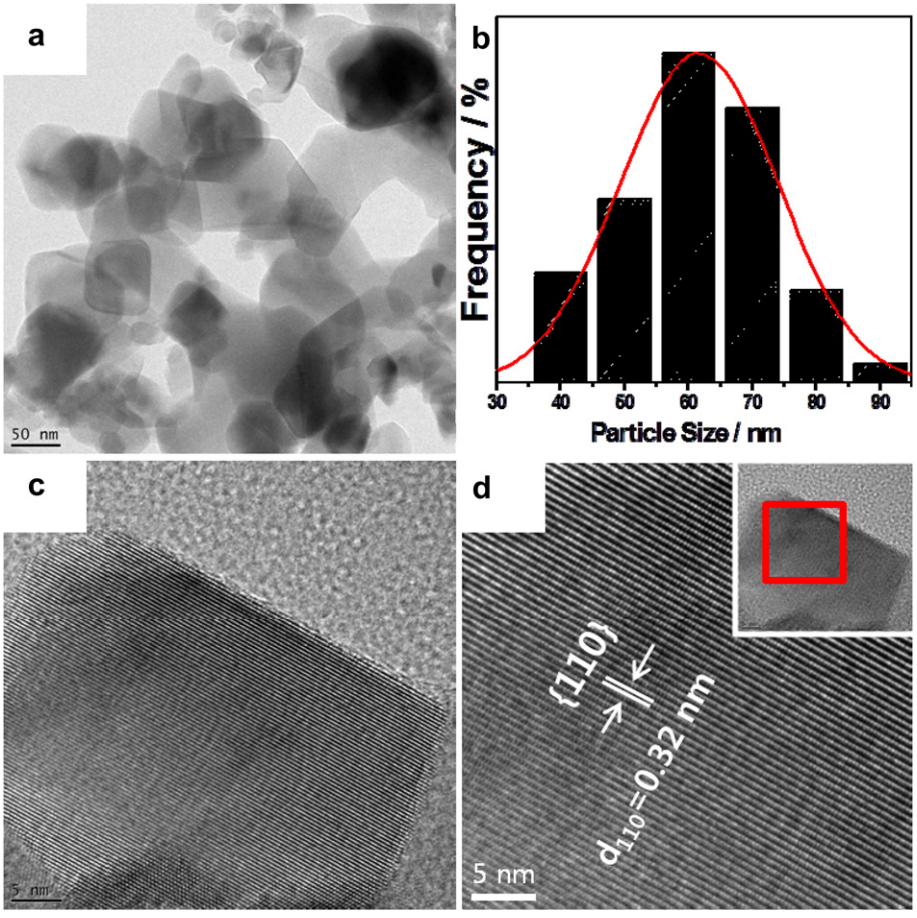

Fig. 3. (a) TEM image and (b) Size-distribution histogram of TiO_2 NPs. (c, d) HR-TEM images of rutile TiO_2 NP.

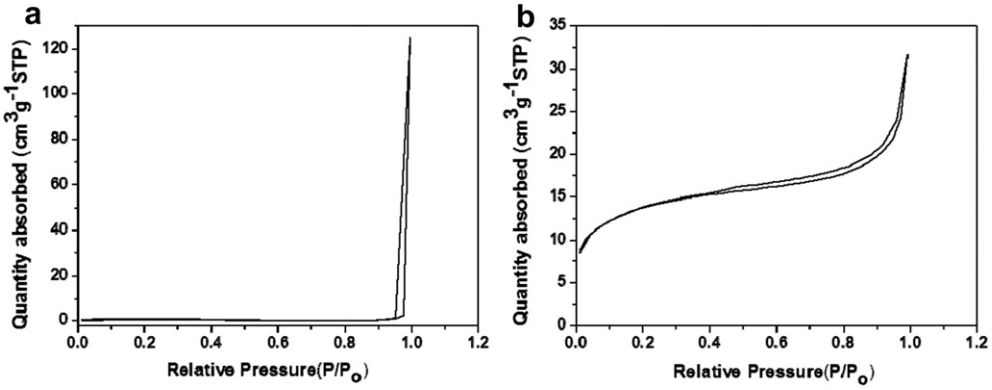

Fig. 4. Nitrogen adsorption/desorption isotherms of (a) TiO_2-NPs and (b) TiO_2-NWs.

represents the rutile phase with tetragonal crystal structure ($a = b = 0.452$ nm, $c = 0.294$ nm) (Fig. 2(a)) The unit cell parameters for TiO_2-NWs are in agreement with those of the bulk TiO_2 rutile phase with space group of P42/mnm (JCPDS No. 88-1175). The lithium intercalation properties of TiO_2-NWs were compared with TiO_2 nanoparticles (TiO_2-NPs) prepared by heating commercial TiO_2 (Degussa P25) at 800 °C in air atmosphere. Typically, the commercial TiO_2 consists of dominant anatase and rutile phase. In general, it is known that the phase transformation from metastable anatase to stable rutile occurs at over 600 °C. In the present case, it can be observed that the anatase phase is completely transformed into the rutile phase at 600 °C. The as-prepared TiO_2-NPs exhibit rutile phase with an average particle size of ~60 nm (Fig. 2(b) & Fig. 3). Furthermore, to characterize surface area of the nanostructured TiO_2, the Brunauer–Emmett–Teller (BET) curves were obtained using TiO_2-NPs and TiO_2-NWs as shown in Fig. 4. The BET specific surface area of TiO_2-NWs is 46.0 $m^2\ g^{-1}$ and is much larger than that of TiO_2-NPs (2.0 $m^2\ g^{-1}$).

Fig. 5(a) and (b) show 1st and 2nd discharge-charge curves of TiO_2-NWs at a current density of 1 C as compared to TiO_2-NPs. At the cycling rate of 1 C, the first charge capacities of TiO_2-NWs and TiO_2-NPs are 310 and 115 mAh g^{-1}, respectively. The second charge capacities of TiO_2-NWs and TiO_2-NPs are 204 and 55 mAh g^{-1}, respectively, representing irreversible intercalation properties. The initial discharge capacity of TiO_2-NWs is much larger than those of the previously reported rutile TiO_2 electrodes [27,28]. It can be found that there was voltage plateaus in the discharge curves, which might be attributed to the irreversible change in the structure of the TiO_2 [21,28]. The cycling performance of TiO_2-NWs and TiO_2-NPs at a current rate of 1 C is indicated in Fig. 5(c) and (d). The TiO_2-NWs have much improved performance up to 100 cycles with

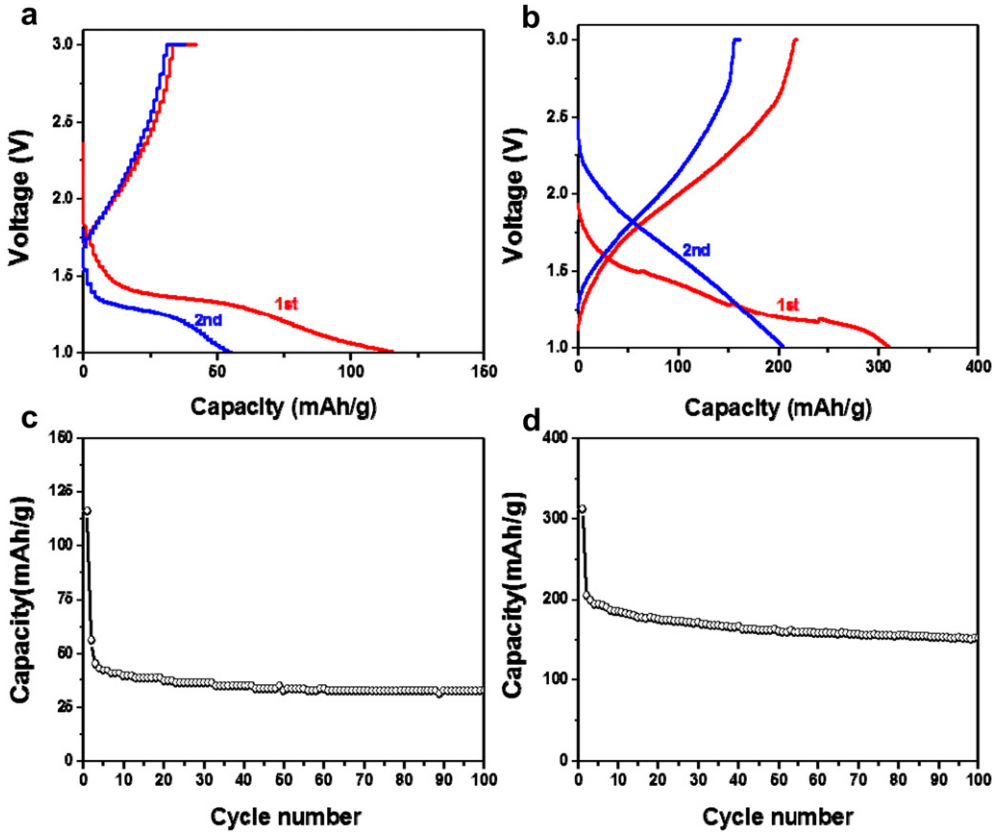

Fig. 5. Charge/discharge curves of (a) TiO_2-NPs and (b) TiO_2-NWs at a current density of 1 C. Cycling performance of (c) TiO_2-NPs and (d) TiO_2-NWs at 1 C for 100 cycles.

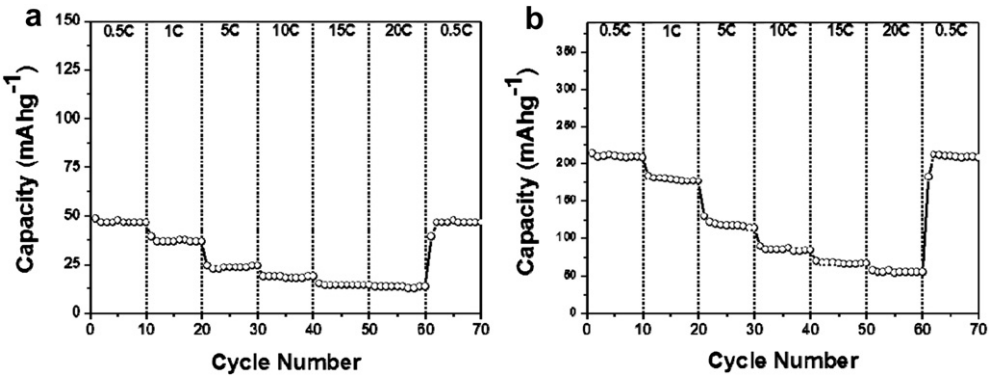

Fig. 6. High-rate capability of (a) TiO_2-NPs and (b) TiO_2-NWs from 0.5 C to 20 C.

a reversible capacity of 173 mAh g^{-1}, compared to that of TiO_2-NPs (36 mAh g^{-1}).

To investigate high-rate cycling performance of the electrodes, the discharge–charge rates were increased stepwise from 0.5 to 20 C. As indicated in Fig. 6(a) and (b) the specific charge capacities of TiO_2-NWs and TiO_2-NPs are 210 and 47 mAh g^{-1} at 0.5 C; 117 and 23 mAh g^{-1} at 5 C; 55 and 13 mAh g^{-1} at 20 C. This represents that even at high current rates from 5 to 20 C, TiO_2-NWs can display an excellent high-rate performance. The remarkably large capacity of 209 mAh g^{-1} can be obtained when the current rate is returned to 0.5 C after 60 cycles at different current rates. The improved lithium-ion intercalation properties of TiO_2-NWs may be attributed to relatively large specific surface area, short transport distance of 1-D nanostructure, and freedom for volume change accompanied by lithium-ion intercalation [27,28].

4. Conclusions

Using hydrothermal process without any surfactant and template, we have prepared TiO_2-NWs with enhanced lithium intercalation properties. The as-prepared TiO_2-NWs exhibit the single-crystalline nature and crystal growth along the [001] direction. The single-crystalline TiO_2-NWs display higher charge capacity and excellent high-rate performance compared to typical rutile TiO_2-NP, facilitating lithium ion motion in the 1D nano-structure electrode.

Acknowledgments

This work was supported by the IT R&D program of MKE/KEIT [KI002176, Development of 3.6Ah Class Cylindrical Type Lithium Secondary Battery] and the Human Resources Development of the Korea Institute of Energy Technology Evaluation and Planning (KETEP) grant funded by the Ministry of Knowledge Economy, Republic of Korea (No. 20104010100610).

References

[1] J.M. Tarascon, M. Armand, Nature 414 (2001) 359.
[2] M.S. Whittingham, Chem. Rev. 104 (2004) 4271.
[3] Y.K. Zhou, L. Cao, F.B. Zhang, B.L. He, H.L. Li, J. Electrochem. Soc. 150 (2003) A1246.
[4] M. Grätzel, Nature(London) 414 (2001) 338.
[5] J.W. Xu, C.H. Jia, B. Cao, W.F. Zhang, Electrochim. Acta 52 (2007) 8044.
[6] A.L. Linsebigler, G.Q. Lu, J.T. Yates, Chem. Rev. 95 (1995) 735.
[7] M.A. Fox, M.T. Dulay, Chem. Rev. 93 (1993) 341.
[8] M.S. Chen, D.W. Goodman, Science 306 (2004) 252.
[9] A. Kuhn, R. Amandi, F. Garcia-Alvarado, J. Power Sources 92 (2001) 221.
[10] P. Segovia, D. Purdie, M. Hengsberger, Y. Baer, Nature 402 (1999) 504.
[11] A.S. Nair, S.Y. Yang, Z. Peining, S. Ramakrishna, Chem. Commun. 46 (2010) 7421.
[12] D.J. Hornbaker, S.-J. Kahng, S. Misra, B.W. Smith, A.T. Johnson, E.J. Mele, D.E. Luzzi, A. Yazdani, Science 295 (2002) 828.
[13] A.I. Hochbaum, P.D. Yang, Chem. Rev. 110 (2010) 527.
[14] B. Liu, E.S. Aydil, J. Am. Chem. Soc. 131 (2009) 3985.
[15] D.V. Bavykin, J.M. Friedrich, F.C. Walsh, Adv. Mater. 18 (2006) 2807.
[16] A. Kumar, A.R. Madaria, C.W. Zhou, J. Phys. Chem. C 114 (2010) 7787.
[17] Y.M. Li, X.J. Lv, J.H. Li, Appl. Phys. Lett. 95 (2009) 113102.
[18] A. Mohammadpour, P.R. Waghmare, S.K. Mitra, K. Shankar, ACS Nano 4 (2010) 7421.
[19] J. Li, W. Wan, H.H. Zhou, J.J. Li, D.S. Xu, Chem. Commun. 47 (2011) 3439.
[20] Y.F. Wang, M.Y. Wu, W.F. Zhang, Electrochim. Acta 53 (2008) 7863.
[21] Z.S. Hong, M.D. Wei, T.B. Lan, L. Jiang, G.Z. Cao, Energy Environ. Sci. 5 (2012) 5408.
[22] Z.R. Tian, J.A. Voigt, J. Liu, B. Mckenzie, H.F. Xu, J. Am. Chem. Soc. 125 (2003) 12384.
[23] S.H. Kang, S.-H. Choi, M.-S. Kang, J.-Y. Kim, H.-S. Kim, T. Hyeon, Y.-E. Sung, Adv. Mater. 20 (1) (2008) 54.
[24] M. Law, L.E. Greene, J.C. Johnson, R. Saykally, P. Yang, Nat. Mater. 4 (2005) 455.
[25] W.J. Li, E.W. Shi, Z.W. Yin, J. Cryst. Growth 208 (1–4) (2000) 546.
[26] B. Liu, D. Deng, J.Y. Lee, E.S. Aydil, J. Mater. Res. 25 (2010) 1588.
[27] C.H. Sun, X.H. Yang, J.S. Chen, Z. Li, X.W. Lou, C.Z. Li, S.C. Smith, G.Q. Lu, H.G. Yang, Chem. Commun. 46 (2010) 6129.
[28] Y.S. Hu, L. Kienle, Y.G. Guo, J. Maier, Adv. Mater. 18 (2006) 1421.